# DUCTILE CONCRETE WALLS WITH STEEL ENDS

**Soon Ho CHO[1], Li Hyung LEE[2], Bryce TUPPER[3] And Denis MITCHELL[4]**

## SUMMARY

Alternative construction techniques incorporating structural steel as the boundary elements in ductile flexural concrete walls are proposed. Two wall specimens containing rectangular hollow structural sections (HSS) and channels at their ends respectively, and one standard reinforced concrete wall specimen were constructed and tested under reversed cyclic loading to evaluate the performance of this new type of construction. The response characteristics and constructibility of these three walls are presented and compared. Three walls showed similar hysteretic properties, but in those with steel ends local buckling of the corresponding structural steel elements following from the significant yielding was observed. Some design recommendations for ductile concrete walls with steel boundary elements are given considering of local instability of structural steel.

## INTRODUCTION

Ductile flexural concrete walls require a significant amount of confining reinforcement at their boundaries to improve the deformation capacity. However, this often causes serious difficulty in the bar placement due to the very smaller spacing required. Replacing the conventional reinforcement by the structural steel in such heavily reinforced regions has many advantages. These include the reduction of on-site labor related to the bar placement, easy connection to steel frames in case of mixed construction, and steel ends also acting as the permanent formwork[NHERP, 1997]. In addition, some inherent properties of composite members such as the increased stiffness and energy absorption are also expected, but not yet fully confirmed[Wakabayashi, 1986]. Thus, this research aims at investigating the reversed cyclic loading responses of alternative construction techniques, incorporating structural steel boundary elements interconnected to the reinforced concrete web of the wall, by comparisons with those of ordinary concrete walls with conventional reinforcement details.

## TEST SPECIMENS

Three half scale test specimens from a twelve storey prototype structure were designed and detailed according to the requirements of the force modification factor, R=3.5 in the Canadian Concrete and Steel Codes[CSA A23.3 and S16.1, 1994]. At an initial stage, the details of three walls were carefully chosen such that all of the walls had approximately the same flexural capacity. The complete interaction between structural steel and concrete in composite wall specimens was also ensured. Due to the available testing apparatus, the wall specimens were tested in their horizontal positions as shown in Fig. 1. Two pairs of 250 mm stroke hydraulic jacks were used to provide the reversed cyclic loading at a distance of 3750 mm from the wall base. The constant axial load of 600 kN corresponding to approximately 11% of the gross sectional concrete strength was provided with four hydraulic jacks and four 15 mm diameter prestressing strands. A steel frame near the tip of the wall was also used to prevent out-of-plane movement of the wall.

Figure 2 shows the overall and cross-sectional dimensions, and structural steel and reinforcement details of the three test specimens. The cross-sectional dimensions of each wall were 1000 mm by 152 mm, with the wall cantilevering 3900 mm from the end foundation block. Specimen W1 used rectangular hollow structural sections (HSS) as boundary elements, which were connected to the wall by welding the transverse bars directly to both HSS elements. HSS sections were not filled with concrete. Specimen W2 connected steel channels to the wall with headed studs, which were welded to the channels and overlapped 175 mm with the transverse reinforcing

[1] Department of Architectural Engineering, Kwangju University, Kwangju, Korea Email: gaza@hosim.kwangju.ac.kr
[2] Department of Architectural Engineering, Hanyang University, Seoul, Korea
[3] Department of Civil Engineering and Applied Mechanics, McGill University, Montreal, Canada
[4] Department of Civil Engineering and Applied Mechanics, McGill University, Montreal, Canada

bars having headed ends of 37 mm x 37 mm x 9.5 mm plates. Specimen W3 is a companion test that meets the requirements of a standard reinforced concrete ductile flexural wall. The confining ties were spaced at a distance of one half the wall thickness, 76 mm, in the plastic hinge region and were spaced at 152 mm elsewhere.

The construction sequence of Specimen W1 was to drill holes in the HSS elements first, then place the bars and align the steel sections, and finally weld to the transverse bars. In Specimen W2, the transverse bars were fabricated by welding plates to their ends resulting in headed bars, 930 mm in length. Standard stud welding procedures were used, which enabled the rapid welding of the studs to the channel boundary elements.

The properties of the Grade 400 reinforcing bars meeting the requirements of CSA G30.18[1992] are presented in Table 1, and also those of the two types of structural steel and the studs meeting the requirements of CSA G40.21[1992] are summarized in Table 2. According to the ratios of width-to-thickness in flanges and height-to-thickness in webs, the flange of a HSS and the web of a channel are more susceptible to local buckling. The effective slenderness ratios are a function of transverse reinforcement or shear connector spacing, $s_h$. The average concrete strengths used for Specimen W1, W2 and W3 were 25.8 Mpa, 38.1 Mpa and 38.7 Mpa respectively.

Load cells were used to measure the positive and negative shear forces on each wall and to monitor the axial load. A number of linear voltage differential transducers (LVDTs) were used to measure the deflections at various locations of each wall. Two LVDTs were used to monitor the tip deflections and two sets of four LVDTs

**Table 1 Properties of reinforcing steel**

| Bar size | Bar description | $f_y$, Mpa | $\varepsilon_y$, mm / mm | $f_{ult}$, Mpa |
|---|---|---|---|---|
| 6 mm diameter | W3 confining hoops | 381.2 | 0.00174 | 445.2 |
| No. 20 | W3 flexural reinforcement | 450.1 | 0.00246 | 610.0 |
| No. 10 | Distributed reinforcement | 487.8 | 0.00285 | 597.5 |

**Table 2 Properties of structural steel**

| Property | Specimen W1 | Specimen W2 |
|---|---|---|
| Steel Description (Area, $mm^2$) | HSS 152x102x6.4 (2960) | C 150x19 (2450) |
| $F_y$, Mpa | 377.0 | 402.2 |
| $\varepsilon_y$, mm/mm | 0.00500 | 0.0028 |
| $F_{ult}$, Mpa | 442.5 | 555.0 |
| Flange b/t ratio = (b-2t)/t | 21.9 | 12.1 |
| CSA Class 1 Flange*, b/t limit | 21.6 ( $420/\sqrt{F_y}$ ) | 20.9 ( $420/\sqrt{F_y}$ ) |
| Web h/w ratio | 14.1 | 6.2 |
| CSA Class 1 Web*, h/w limit | 21.6 ( $420/\sqrt{F_y}$ ) | 7.2 ( $145/\sqrt{F_y}$ ) |
| $s_h$, mm | 180 | 220 |
| Effective slenderness ratio = $s_h/t$ | 28.3 | 19.3 |
| Studs in Specimen W2 (12.7mm diameter and 207mm length) | | |
| $F_y$, Mpa | 402.0 | |
| $F_{ult}$, Mpa | 500.7 | |

*flange and web are longer and shorter elements respectively

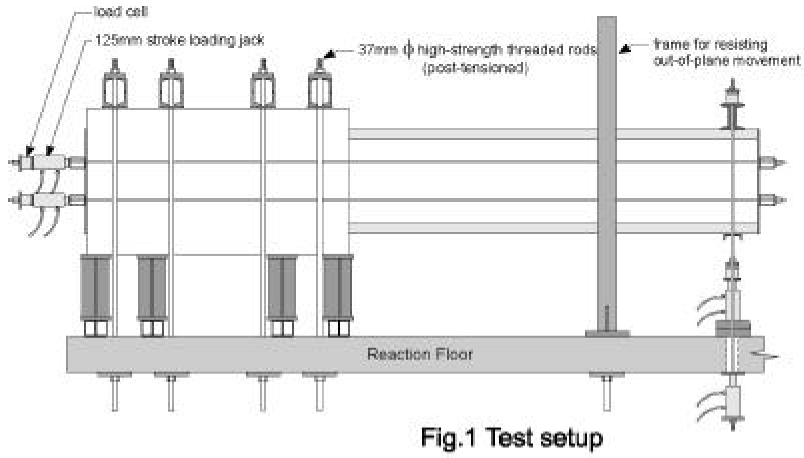


Fig.1 Test setup

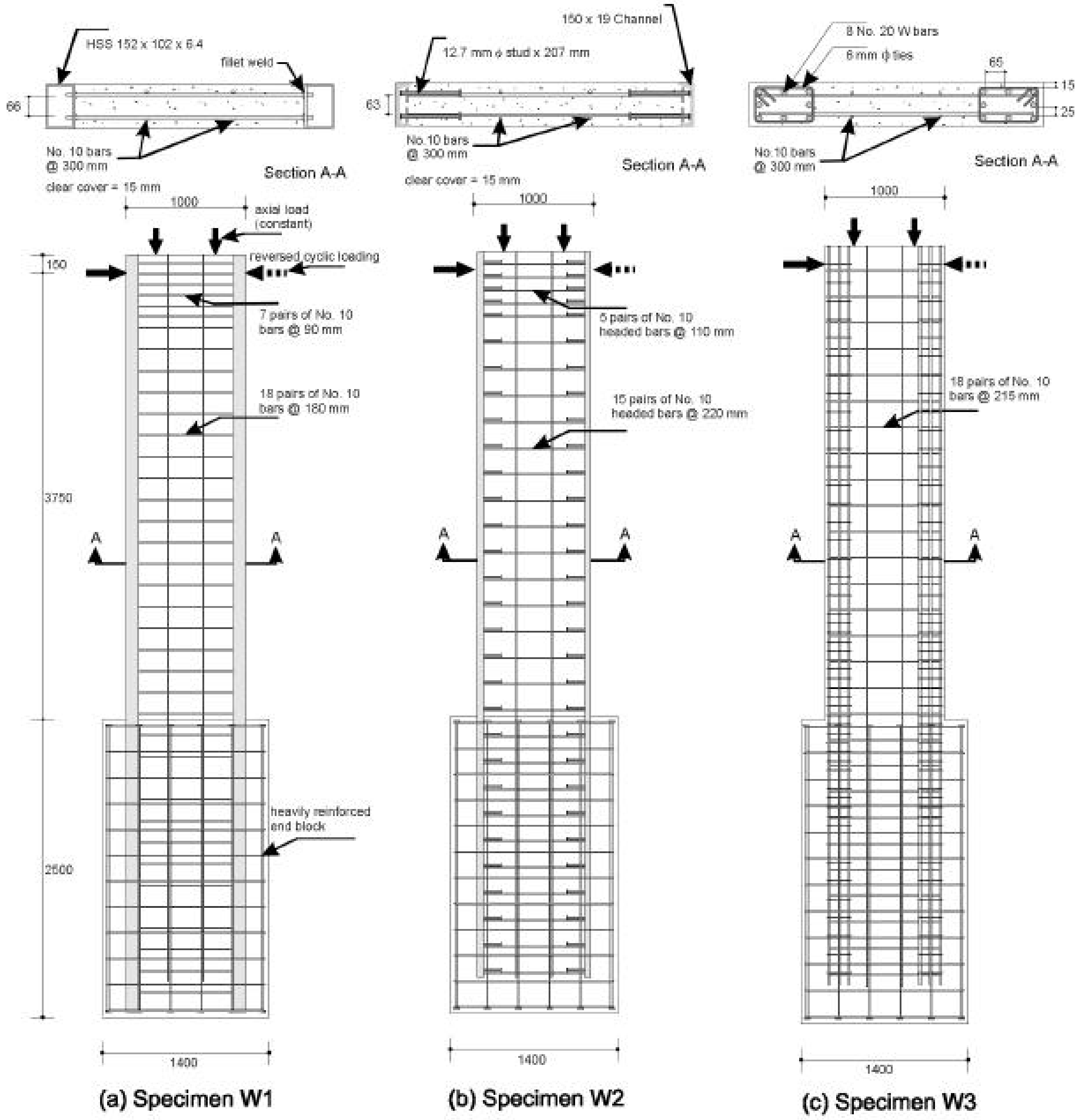


Fig. 2 Details of test specimens

were attached to the tension and compression chords along the height of each wall in order to determine curvatures. Each wall also had LVDTs configured to form a rosette over the length of the expected plastic hinge region. Strain measurements were collected using both electrical resistance strain gauges and demountable mechanical targets. Two rosettes composed of mechanical targets with 200 mm gauge lengths were attached to the concrete in the plastic hinge region. Specimens W1 and W2 had mechanical targets attached to the structural steel and concrete in order to measure any separation between them. Seven strain gauges were placed on the outer faces of the tension and compression steel chords, or the No. 20 reinforcing bars of each wall. These allowed the progression of yielding along the height of each wall to be monitored. Additional strain gauges with 2 mm gauge lengths were also placed on specific transverse reinforcement in each wall.

Loading was applied to predetermined load levels up to the general yielding. The first cycle was to produce the precalculated moment, $0.5M_{cr}$, equal to half of the cracking moment. The second cycle loaded the walls to the theoretical cracking moment, $M_{cr}$. The next cycle was determined by the first yielding of flexural steel in the wall, monitored by the electrical resistance strain gauges. The peak of the fourth cycle was taken as the load and deflection corresponding to general yield, $\Delta_y$, of the wall. The cycles after general yielding were controlled by deflection limits, based on multiples of the general yield deflection.

## TEST RESULTS

Figure 3 shows the base moment vs. wall tip deflection responses for the three specimens, indicating similar hysteretic behaviour. The first yielding of Specimen W1 occurred during the positive loading cycle 3A at a base shear of 191.2 kN and a corresponding deflection of 22 mm(see Fig. 3a). General yielding also occurred during this loading cycle at a base shear of 257.5 kN and a deflection of 36.6 mm. The crack development during this stage was significant with many flexural cracks forming perpendicular to the concrete and HSS interface at the location of each transverse reinforcing bar. During the fourth cycle, crushing of the concrete near the compression face of the wall occurred, and during the fifth cycle, local buckling began in the outer flange(see Fig. 4a). During cycle 6, approximately three time the general yielding deflection, the HSS experienced further buckling of the compression side and pullout from the end block on the tension side. The final half-cycle, 7A, was an attempt to reach beyond the previous 100 mm deflection. However, at 98.8 mm a sudden reduction in load occurred as the bottom HSS completely buckled, brought on by excessive crushing of the concrete (see Fig. 5a).

In Specimen 2, the first yielding occurred during the negative loading cycle 4B at a base shear of 279.8 kN and a corresponding deflection of 30.9 mm. General yielding occurred in the positive loading cycle at 34.3 mm and in the negative loading cycle at a deflection of 33.7 mm. As can been seen from Fig. 3b, first yielding and general yielding are very close together. During cycle 6, horizontal cracks formed along the steel and concrete interface, parallel to the steel sections, indicating that some separation was taking place. During the seventh cycle, significant cracking and the first noticeable concrete crushing occurred close to the base of the wall. Also noticeable during this cycle was a 2 mm pullout of the tensile steel section, relative to the end block. During cycle 8, channel yielding was indicated by surface flaking of the mill scale over a length of 580 mm, originating from the base of the wall. At the peak loading of 9A, yielding of the tensile channel had propagated to 790 mm from the wall base and local buckling was first noticed in the compression channel. The local buckling began as outward buckling of the flanges followed by the webs(see Fig. 4b). In addition, during cycle 9, concrete crushing and some spalling was evident along with the development of several large shear cracks. Specimen W2 failed on the positive loading of the tenth cycle when the compression loaded channel underwent local buckling, 50 mm from the base of the wall (see Fig. 5b).

The first yielding of Specimen W3 was estimated to have occurred just before the peak of cycle 4A at a base shear level of 251.2 kN and corresponding tip deflection of 28 mm (see Fig. 3c). This stage also corresponded to compression yielding of the lower No. 20 reinforcing bars. General yielding during the positive loading occurred at a deflection of 35.8 mm, at the peak of the fifth cycle. By this stage, the crack patterns of Specimen W3 were significantly different from the crack patterns of Specimens W1 and W2 (see Fig. 4c). At the wall ends, in the area of the concentrated longitudinal reinforcement, there were a large number of closely spaced small cracks. Moreover, the shear crack widths in cycle 6 reached a maximum of only 0.4 mm. During the seventh cycle, several shear and flexural cracks merged, while concrete crushing began in the compression zone. Cycle 8 did not reach the same peak loads as the previous cycles, which was most likely due the concrete crushing. At this stage, the maximum width of the shear cracks was measured at 1.5 mm. In the last full cycle before failure, cycle 9, further widening of the cracks occurred along with continued concrete crushing. Specimen W3 failed abruptly during the positive loading of the tenth cycle at a load of 317.1 kN and a tip deflection of 114 mm. It is evident from Fig. 5c that failure occurred due to severe distress in the compression zone with concrete crushing, rupturing of one of the confining hoops and local buckling of the longitudinal bars.

## ANALYSIS AND COMPARISON OF RESPONSES

The analysis of the reversed cyclic responses, behavioural comparisons and a discussion of the differences in the construction techniques for the three wall specimens are presented. The construction of concrete walls with steel boundary elements proved to have several advantages. Among them, the major advantage is that considerable prefabrication is possible, reducing the on-site labour and hence reducing construction time. Specimen W1 required a significant amount of welding and drilling which necessitated more labour than was needed for Specimen W2. Combining studs and prefabricated headed reinforcing bars was a concept that made Specimen W2 a reasonable alternative to conventional construction.

Figure 6 presents the moment vs. curvature responses, determined from the curvatures measured near the base and the corresponding moments for each wall. Monotonic responses for each wall were also predicted using the computer programs RESPONSE [Collins and Mitchell, 1991]. The cross-section of each wall was discretized into ten concrete layers with the boundary elements simulated by several steel layers. The full non-linear responses of both the concrete and the steel, including strain hardening and confining effects were modeled[Mander et al., 1988]. The predicted curvatures are very close to the envelope of the experimental results. Table 3 summaries the predicted plastic hinge lengths determined from the assumed curvature distribution at ultimate stages and length of tension steel yielding determined from the electrical resistance strain gauges for three specimens. It must be noted that the actual plastic hinge length is somewhat less than the length over which yielding of the tension steel was recorded.

The hysteretic responses of the wall specimens are described using comparisons of the displacement ductility, ability to increase load beyond general yielding, peak-to-peak stiffness degradation and cumulative energy absorption. Table 4 summarizes the maximum values of each of these attributes and indicates the failure mode of each specimen. The deflection ductility is taken as the ratio of the ultimate positive tip deflection, $\Delta_u$, to the positive tip deflection at general yield, $\Delta_y$. The $V_u/V_y$ ratio indicates a specimen's ability to increase its load and maintain the load after general yielding. $V_u$ and $V_y$ represent the loads corresponding to $\Delta_u$ and $\Delta_y$ respectively. The third parameter, $k_u/k_y$, represents the stiffness degradation between general yielding and ultimate deflection. The stiffnesses, $k_u$ and $k_y$, represent the slope of the line joining the peaks of the respective positive and negative load-deflection responses. The cumulative energy dissipation is obtained by integrating the areas under the load-deflection curves and hence is representative of the hysteretic damping.

All three specimens have comparable displacement ductility, averaging about 3.0. Also, Table 4 and Fig. 7a show that Specimen W1 reached the largest value of $V_u/V_y$, since the response of this wall was governed by the structural steel. These tension and compression chords experienced significant strain hardening allowing Specimen W1 to maintain the load in the later stages. Specimen W2 began to lose its capability to sustain load in the last full cycle due to concrete crushing and buckling of the channel in compression. Specimen W3, after yield, maintained a constant $V_{peak}/V_y$ ratio of approximately 1.1.

**Table 3 Predicted plastic hinge lengths and experimental yielding lengths**

| Specimen | $M_y$, KN·m | $M_u$, kN·m | $\ell_p$, mm | Yielding length, mm (from tests) |
|---|---|---|---|---|
| W1 | 986.5 | 1253.4 | 798 | 1200 |
| W2 | 1079.8 | 1305.2 | 647 | 800 |
| W3 | 1109.2 | 1285.0 | 513 | 750 |

**Table 4 Summary of specimen responses**

| Specimen | Mode of failure | $\Delta_u/\Delta_y$ | $V_u/V_y$ | $k_u/k_y$ | Energy, N·m |
|---|---|---|---|---|---|
| W1 | HSS local buckling | 2.80 | 1.27 | 0.42 | 71.0 |
| W2 | Channel local buckling and concrete crushing | 3.0 | 1.03 | 0.36 | 87.1 |
| W3 | Concrete spalling and crushing followed by bar buckling and rupture of confining tie | 3.18 | 1.08 | 0.47 | 70.6 |

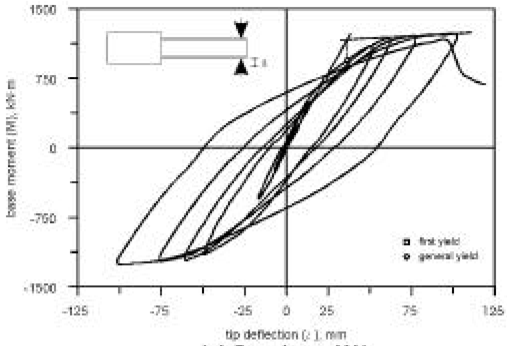


(a) Specimen W1

(a) Specimen W1

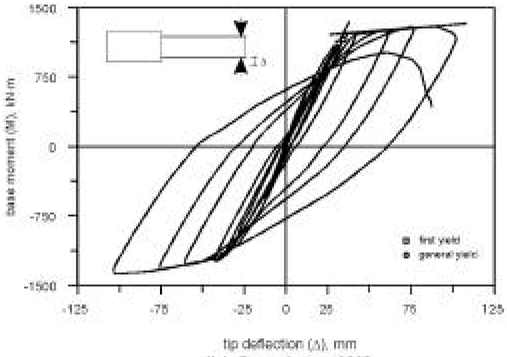


(b) Specimen W2

(b) Specimen W2

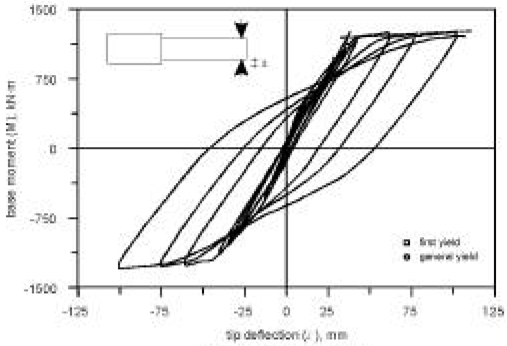


(c) Specimen W3

(c) Specimen W3

Fig. 4 Crack patterns and failure modes

Fig. 3 Moment vs. deflection responses

(a) (b) (c)

Fig.5 Close-up views of failure regions

The ultimate stiffness ratios in Table 4 show that all of the specimens had a similar peak-to-peak stiffness ratio, $k_u/k_y$, at the end of their respective tests. Figure 7b illustrates the stiffness degradation of each specimen throughout the entire test. The most evident difference between the specimens is the significantly lower initial stiffness of Specimen W1. Although Specimen W1 had comparable flexural strength to that of the other specimens its elastic stiffness was less due to the HSS being remained hollow. Figure 7c compares the cumulative energy dissipation versus ductility for each wall. It is shown that Specimen W2 dissipated the greatest amount of energy, approximately 25% more energy than the other two specimens. The greater cumulative energy dissipation of Specimen W2 is due to the properties of structural steel and the full filling of concrete to the interior of channels.

## STRUCTURAL STEEL LOCAL BUCKLING

Various types of structural steel sections such as wide-flange, angle, channel and HSS can be used for the chord members of composite walls. An HSS is one of the most economical sections because it is capable of developing large compressive strains. This is due to a larger radius of gyration when compared with other sections with the same cross sectional areas. However, there are concerns about the ductility of HSS brace members after local buckling occurs. HSS members serving as truss chords in a composite wall are expected to be subject to much less severe strain gradients over their depth. As described in Table 2, the width-to-thickness ratios in flanges and the height-to-thickness ratios in webs of the structural steel used all satisfy the requirements for Class 1 sections in the CSA S16.1 Standard[1994]. The strain measurements on the steel sections included local strain measurements using electrical resistance strain gauges and average strain measurements using LVDTs. The electrical resistance strain gauges were typically located just outside of the regions of most severe local buckling, however the LVDT readings captured the average strains across these regions. From the strain readings the following conclusions were made: 1) Initial signs of local buckling are apparent at strains of about 1%, 2) Both the HSS and the channel sections had strains greater than 2% and hence it is assumed that strain hardening was achieved prior to local buckling. These reversed cyclic loading tests have indicated that in order for composite walls to get comparable behaviour to a reinforced concrete ductile flexural wall, Class 1 sections must be used, since local buckling must be delayed until reasonably high strains are reached. Another important aspect in the design is to provide adequate connection between the steel section and the concrete. The provision of a sufficient number of discrete shear connectors, such that their shear capacity would enable yielding of the HSS chord member, was found to be essential in achieving ductile response. This also results in the reduced effective slenderness ratio, $s_h/t$.

## DESIGN RECOMMENDATIONS AND CONCLUSIONS

1) The hysteretic responses of composite walls with boundary elements were very similar to that of a typical reinforced concrete ductile flexural wall when all of the walls were designed to have equivalent flexural capacities. Composite wall Specimen W2 exhibited slightly better energy dissipation than the other two specimens.
2) The welding of transverse reinforcing bars directly to the hollow structural steel tubes in Specimen W1 provided excellent shear connection enabling the full development of yielding of the boundary elements. The shear connection in Specimen W2, consisting of studs welded to the steel channels together with overlapping headed transverse bars, proved capable of developing the full yield of the steel channels. However, significant separation occurred between the steel channel and the reinforced concrete web.
3) The failure mode of composite walls was precipitated by local buckling of the structural steel boundary elements. While a more compact steel section and a reduced spacing of shear connection in the plastic hinge region would help control local buckling, both composite walls achieved ductilities and energy absorption comparable to the reinforced concrete ductile flexural wall.
4) The positioning of channels in Specimen W2 provided some concrete confinement at both ends of the wall. The placement of the hollow steel sections at the extreme ends of Specimen W1 enabled this wall to resist flexure almost entirely by forces in the structural steel chords.
5) The use of prefabricated elements in the construction of the boundary element walls would significantly reduce on-site labour. The construction of Specimen W1 required more care during prefabrication of the reinforcement than Specimen W2. However, Specimen W2 requires more on-site placement of reinforcement than Specimen W1. Due to the intricate details of the confinement reinforcement at the ends of Specimen W3, this specimen requires the greatest amount of on-site labour.

## ACKNOWLEDGEMENTS

The authors would like to acknowledge STRESS, a nationwide research center in Korea supported by KOSEF (Korean Science and Engineering Foundation) for funding this collaborative research project between STRESS and Concrete Canada.

## REFERENCES


Building Seismic Safety Council (1997), NEHRP Recommended Provisions for Seismic Regulations for New Buildings and Other Structures, Washington, D.C.

Canadian Standards Association (1992), CAN/CSA-G30.18 - Billet Steel Bars for Concrete Reinforcement, Rexdale, Ontario.

Canadian Standards Association (1992), CAN/CSA-G40.21 – General Requirements for Rolled or Welded Structural Quality Steel, Rexdale, Ontario.

Canadian Standards Association (1994), CSA Standard A23.3-94 - Design of Concrete Structures, Rexdale, Ontario.

Canadian Standards Association (1994), CAN/CSA-S16.1 - Limit States Design of Steel Structures, Rexdale, Ontario.

Collins, M.P., and Mitchell (1997), D., Prestressed Concrete Structures, Prentice Hall, Toronto/Montreal.

Mander, J. B., Priestley, M. J. N., and Park R. (1988), "Theoretical Stress-Strain Model for Confined Concrete", *ASCE Journal of Structural Engineering*, Vol. 114, No. 8, August, pp.1804-1827.

Wakabayashi, M (1986), Earthquake-Resistant Buildings, McGraw-Hill, New York.


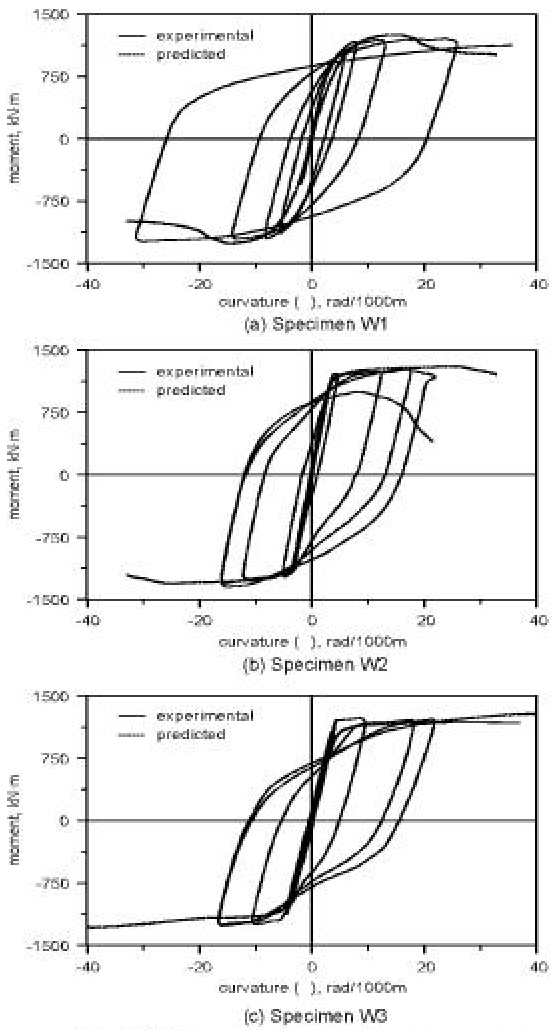


**Fig. 6 Moment vs. curvature responses**

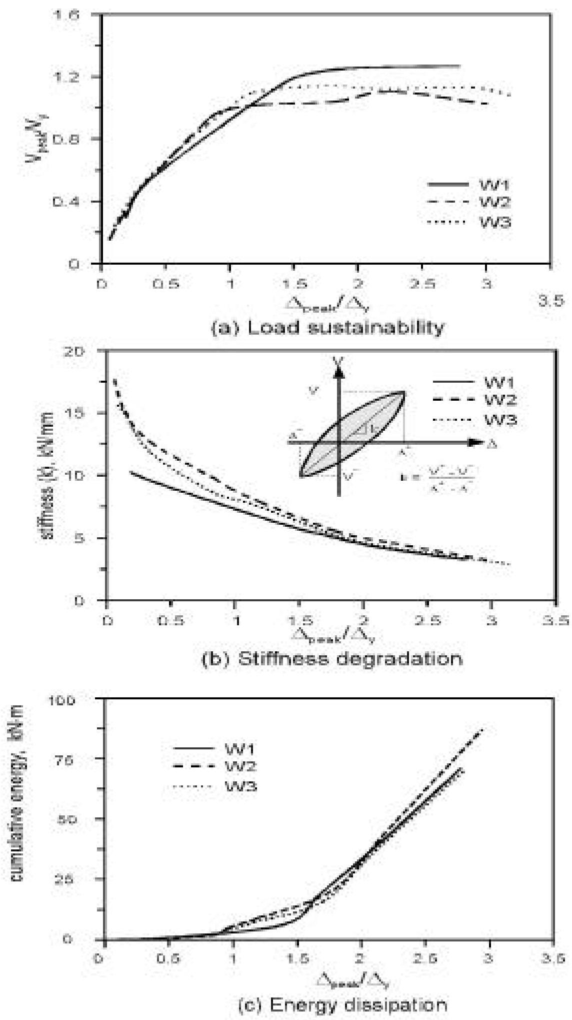


**Fig. 7 Hysteretic responses**